

# *Ab initio* quantum Monte Carlo calculations of spin superexchange in cuprates: the benchmarking case of $\text{Ca}_2\text{CuO}_3$

Kateryna Foyevtsova,<sup>1</sup> Jaron T. Krogel,<sup>1</sup> Jeongnim Kim,<sup>1</sup>  
P. R. C. Kent,<sup>2</sup> Elbio Dagotto,<sup>1,3</sup> and Fernando A. Reboredo<sup>1</sup>

<sup>1</sup>*Materials Science and Technology Division, Oak Ridge National Laboratory, Oak Ridge, TN 37831, USA*

<sup>2</sup>*Center for Nanophase Materials Sciences and Computer Science and Mathematics Division,  
Oak Ridge National Laboratory, Oak Ridge, TN 37831, USA*

<sup>3</sup>*Department of Physics and Astronomy, The University of Tennessee, Knoxville, TN 37996, USA*

(Dated: June 7, 2018)

In view of the continuous theoretical efforts aimed at an accurate microscopic description of the strongly correlated transition metal oxides and related materials, we show that with continuum quantum Monte Carlo (QMC) calculations it is possible to obtain the value of the spin superexchange coupling constant of a copper oxide in a quantitatively excellent agreement with experiment. The variational nature of the QMC total energy allows us to identify the best trial wave function out of the available pool of wave functions, which makes the approach essentially free from adjustable parameters and thus truly *ab initio*. The present results on magnetic interactions suggest that QMC is capable of accurately describing ground state properties of strongly correlated materials.

PACS numbers: 71.15.-m, 02.70.Ss, 74.72.-h, 75.30.Et, 75.47.Lx

For decades, transition metal oxides have been amongst the most intriguing materials due to the complex correlated behavior of the  $3d$  or  $4d$  electrons of a transition metal ion. In particular, strong electronic correlations often give rise to non-trivial magnetism, such as quantum spin-liquid states in low-dimensional Mott insulating oxides. High-temperature superconductivity in copper oxides (cuprates) is also believed to originate from magnetic spin excitations that bind Cooper pairs [1–3]. Electronic correlations, however, also make this class of materials among the most difficult to describe theoretically, both from model as well as *ab initio* perspectives.

One of the practical challenges of *ab initio* electronic structure theory is to accurately predict the strength of magnetic coupling between localized spins of transition metal ions [4]. For solids, a natural method of choice is periodic density functional theory (DFT). DFT gives access to the system's ground state energy corresponding to different configurations of localized spins, which can be mapped onto the eigenstates of the a spin model to extract the magnetic couplings  $J$ . This approach relies on the accuracy of the description of the ground state. Unfortunately, the presently available approximations to the exchange-correlation functional in DFT either poorly account for the exchange and correlation effects [local density approximation (LDA)] or depend on empirical input parameters (LDA+U, hybrid functionals). Often, the only way to find an appropriate approximation for the system of interest is by comparing theoretical calculations with experiment, compromising the predictive nature of such calculations.

This problem is generic to a broad class of transition metal oxides. Let us exemplify the aforementioned limitations of DFT by considering the case of the Mott insulators  $\text{Ca}_2\text{CuO}_3$  and  $\text{Sr}_2\text{CuO}_3$ . These systems are one of the best realizations of the one-dimensional (1D) spin- $\frac{1}{2}$  antiferromagnetic Heisenberg chain model, demonstrat-

ing spin-liquid behavior and separation of spin and orbital degrees of freedom [11]. The crystal structure of  $\text{Ca}_2\text{CuO}_3$  and  $\text{Sr}_2\text{CuO}_3$  is similar to that of the superconducting two-dimensional cuprates, with the difference that in the  $\text{CuO}_2$  plane the oxygen atoms along the crystallographic  $b$  direction are missing, so that the Cu chains run along the  $a$  direction [Fig. 1 (a)]. The Cu-O-Cu bridge provides a favorable path for superexchange coupling between Cu spins, resulting in a particularly strong coupling constant  $J$ . The experimental estimate of  $J$  has been extracted from various probes, performed mostly on  $\text{Sr}_2\text{CuO}_3$ , and ranges between 0.13 and 0.26 eV (see Table I and Ref. 12 for details). Temperature dependent

Method	$J$ (eV)
Experiment [INS]	0.241(11) Ref. 5
Experiment [ $\chi(T)$ ]	0.146(13) Refs. 6 and 7
	0.189(17) Ref. 8
FP-DMC	0.159(14) This work
	0.115(10) This work [9]
Cluster DDCI3	0.231 Ref. 10
UHF	0.04 Ref. 10
LDA	0.64 This work

TABLE I. The nearest-neighbor spin superexchange coupling constant  $J$  of  $\text{Ca}_2\text{CuO}_3$  and  $\text{Sr}_2\text{CuO}_3$  obtained with different theoretical ( $\text{Ca}_2\text{CuO}_3$ ) and experimental ( $\text{Sr}_2\text{CuO}_3$ ) methods. The abbreviations used stand for: INS=inelastic neutron scattering, FP-DMC=fixed-phase diffusion Monte Carlo, DDCI3=difference dedicated configuration interaction with three degrees of freedom, UHF=unrestricted Hartree-Fock, LDA=local density approximation.  $\chi(T)$  denotes a temperature dependent magnetic susceptibility.

magnetic susceptibility measurements, supported by rigorous theoretical modeling [7, 8, 13], narrow this window to 0.15-0.19 eV. Theoretical predictions of  $J$ , in turn, vary drastically by as much as an order of magnitude depending on the method used. For example, periodic DFT with LDA gives 0.64 eV, whereas the periodic unrestricted Hartree-Fock (UHF) method gives 0.04 eV (Table I). In addition, LDA+U calculations give results that depend strongly on  $U$ . Cluster calculations with the configuration interaction method may give a more reasonable result, as in this case (Table I, Ref. 10), but, generally speaking, their applicability to condensed phase systems is intrinsically limited. In view of this, developing a new, more universal and accurate, *ab initio* approach to computing magnetic interactions is critically important. Needless to say, a method capable of accurately describing magnetic interactions in transition metal oxides will also provide an improved *ab initio* description of many other ground state properties of these complex systems, and hence may yield new physical insights.

Here, we apply the diffusion Monte Carlo method [14] within the fixed-phase approximation (FP-DMC) to compute the value of the spin superexchange interaction constant in a transition metal oxide. To the best of our knowledge, this is among the first calculations of magnetic couplings in complex oxides that has been attempted with a method capable of chemical accuracy in full periodic boundary conditions. The fixed-phase error is controlled by scanning over a set of trial wave functions and using the variational nature of DMC energy, as explained below. This way, the variational principle determines the choice of the initial DFT functional to generate a trial wave function and thus eliminates empiricism from the calculations. We choose the 1D cuprate antiferromagnet  $\text{Ca}_2\text{CuO}_3$  as our test system because of the simplicity of its underlying spin model and relatively light constituent atoms, as compared to other cuprates, including  $\text{Sr}_2\text{CuO}_3$ , to minimize the potential role of relativistic effects. Our result for the nearest-neighbor Cu spin coupling,  $J = 0.159 \pm 0.014$  eV [9], is in excellent agreement with the value extracted from the temperature dependence of magnetic susceptibility (Refs. 6–8, Table I).

Historically, quantum Monte Carlo has played a fundamental role in advancing electronic structure theory. Released-node DMC calculations on the homogeneous electron gas by Ceperley and Alder [16] were used to construct the local density approximation to the exchange-correlation functional which is at the core of modern DFT methods. In FP-DMC, the Schrödinger equation is rewritten in a form of an integral diffusion equation, which is stochastically solved via quantum Monte Carlo sampling by iteratively propagating the wave function in imaginary time. As a result, the ground state (GS) wave function is projected out. In order to handle the fermion sign problem, the complex phase of the target GS wave function is fixed to those of an input trial wave function. The fixed-phase approximation introduces a variational

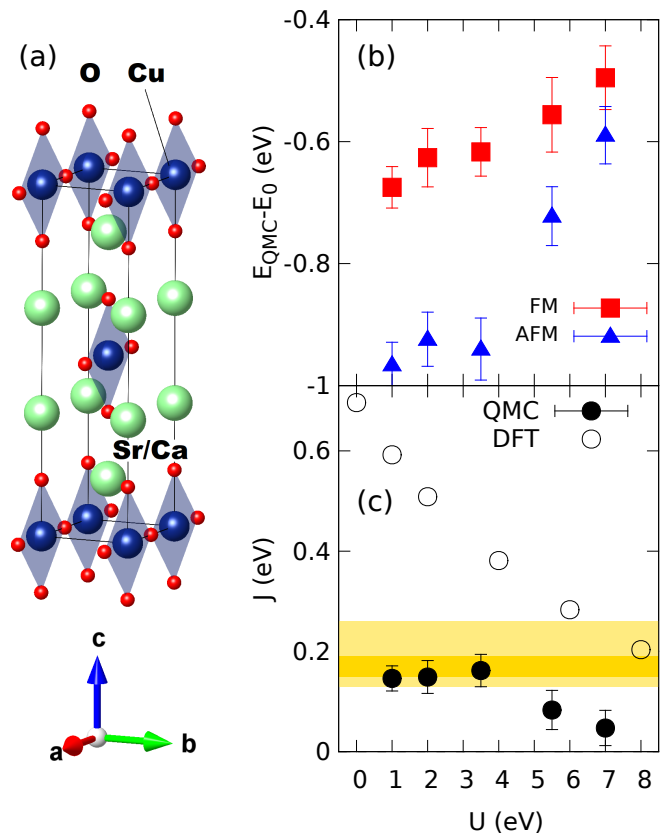


FIG. 1. (a) The conventional “ $1 \times 1 \times 1$ ” unit cell of  $\text{Ca}_2\text{CuO}_3$  and  $\text{Sr}_2\text{CuO}_3$ . For calculations, the unit cell crystallographic parameters reported in Ref. 15 were used. (b) The total energies of the antiferromagnetic and ferromagnetic states of  $\text{Ca}_2\text{CuO}_3$  calculated with FP-DMC as a function of the trial wave function, characterized by the LDA+U parameter  $U$ , used here as a variational parameter. For convenience of presentation the FP-DMC energies are shifted by  $E_0 = 34705$  eV. (c) The nearest-neighbor Cu spin superexchange coupling constant  $J$  of  $\text{Ca}_2\text{CuO}_3$  calculated with WIEN2k (DFT) and FP-DMC as a function of  $U$ . For comparison, the ranges of experimentally determined  $J$  values of  $\text{Sr}_2\text{CuO}_3$  are shown in light gold and dark gold bands. The light gold band represents all reported experimental estimates [12], while the dark gold band represents the magnetic susceptibility measurements [7, 8].

systematic error in the DMC energy which can be assessed and controlled by comparing results obtained with different trial wave functions. Exchange and correlation effects are fully accounted for within the fixed phase approximation. Even though the computational costs of FP-DMC grow as  $N^3$ , where  $N$  is the number of particles, the costs of calculating quantities *per particle* grow only as  $N^2$ , which is a great advantage in the present case since  $J$  is a characteristic of a *Cu-Cu bond*. Due to improvements in algorithms and available computer power, QMC has achieved a growing success in accurately pre-

dicting the properties of complex materials [17–22].

We used the DFT plane-wave code Quantum Espresso [23] in order to self-consistently generate trial wave functions in a single Slater determinant form. The LDA+U method was applied, with the values of the on-site Coulomb repulsion between Cu 3d electrons,  $U$ , varying as 1, 2, 3.5, 5.5, and 7 eV. The energy cut-off was set to 500 Ry due to the use of very hard pseudopotentials and inclusion of semi-core electrons in the valence (described below). The corresponding DMC energies were subsequently compared to determine the best trial wave function. We present results that follow procedures in the literature [24–29] to obtain the spin superexchange coupling constant  $J$ . The coupling constant can be computed from a single total energy difference:  $J = (E_{FM} - E_{AFM}) / (2N_{Cu-Cu}s_z^2)$ . Here  $s_z = 1/2$  is the z-component of an electron’s spin and  $N_{Cu-Cu}$  is the number of nearest neighbor Cu-Cu bonds in a given supercell. This results from a mapping to the total energy differences of an Ising Hamiltonian. The estimate for  $J$  changes somewhat using a different approach [9], though the result remains close to the experimental range. Although the total energies are variational,  $J$  is not and care must be taken to fully optimize the trial wavefunctions. Wavefunctions of the standard spin-assigned Slater-Jastrow type [14] used here are eigenstates of total  $\hat{S}_z$ , but not  $\hat{S}^2$ . Although it is possible to construct eigenstates of  $\hat{S}^2$ , this is seldom done in practice with DMC because the Slater-Jastrow form gives accurate total energies within the fixed-node/phase approximation [30] for spin-independent Hamiltonians. For all considered  $U$  values, both FM and AFM solutions are insulating in DFT.

Fixed phase DMC calculations were performed with QMCPACK [31]. The DMC imaginary time step and the number of walkers have been converged to, respectively, 0.005 Ha<sup>-1</sup> and 2000 per boundary twist (in the  $2 \times 1 \times 1$  supercell). To assess finite size errors we considered  $2 \times 1 \times 1$  ( $N_{Cu-Cu} = 4$ ) and  $2 \times 2 \times 1$  ( $N_{Cu-Cu} = 8$ ) supercells, defined with respect to the conventional *Immm* crystallographic unit cell of Ca<sub>2</sub>CuO<sub>3</sub> [Fig. 1 (a)]. The  $2 \times 1 \times 1$  supercell contains four formula units, *i.e.*, 28 atoms with 228 electrons. We also performed averaging over twisted boundary conditions on a  $2 \times 4 \times 1$   $k$ -point grid for the  $2 \times 1 \times 1$  supercell ( $2 \times 2 \times 1$  for the  $2 \times 2 \times 1$  supercell). The necessity of twist averaging indicates that cluster model calculations, such as those in Ref. 10, are under converged with respect to finite size effects. The ionic potentials were approximated by employing pseudopotentials (PPs). Through an extensive investigation, we have found the inclusion of semi-core electrons to be essential for high quality results. Core sizes used for the pseudopotentials are as follows: He-core for oxygen atoms (6 electrons in valence), Ne-core for calcium atoms (10 electrons in valence), and Ne-core for copper atoms (19 electrons in valence). The quality of the PPs has been carefully tested within both DFT and DMC, as reported in detail in Appendix A.

We first present the FP-DMC results obtained for the  $2 \times 1 \times 1$  supercell, which contains two Cu atoms along the chain direction *a*. Figure 1 (b) displays the FP-DMC total energies of the FM and AFM states as a function of the trial wave function, characterized by the LDA+U parameter  $U$ . In these calculations we stress that the  $U$  is simply a convenient optimization parameter for generating FP-DMC wave functions. Both the FM and AFM curves follow a non-linear  $U$  dependence, reaching minima and leveling off in the region between  $U=1$  and 3.5 eV, within the available statistical resolution.

From the difference between the AFM and FM FP-DMC total energies we compute the spin superexchange constant  $J$ , shown in Fig. 1 (c) together with the respective LDA+U  $J$  values for comparison. Also indicated are the ranges of experimentally determined  $J$  values of Sr<sub>2</sub>CuO<sub>3</sub>: the light gold band represents all reported experimental estimates [12], while the dark gold band represents susceptibility measurements [6–8], which is one of the most reliable probes. Since, unfortunately, no equivalent experimental data on Ca<sub>2</sub>CuO<sub>3</sub> are available, we can only compare our theoretical calculations with the experiments performed on Sr<sub>2</sub>CuO<sub>3</sub>. This is a valid approach as the spin exchange couplings of the two cuprates should differ by no more than a few percent [32]. From Fig. 1 (c), one readily sees that in the  $U$  region between 1 and 3.5 eV, corresponding to the minimal FP-DMC energies in Fig. 1 (b), the FP-DMC results for  $J$  are in good agreement with the susceptibility data, within statistical resolution. In contrast, all electron LDA+U (LAPW) results strongly depend on  $U$ , requiring a large value of  $U \approx 8$  to obtain reasonable  $J$ -values.

We now assess the finite size error associated with these results by performing FP-DMC calculations on a  $2 \times 2 \times 1$  supercell, obtained by doubling the original  $2 \times 1 \times 1$  supercell in the direction perpendicular to the Cu chains. The  $U=3.5$  eV LDA+U trial wave function is used here as the one to provide a good complex phase for FP-DMC, as has been established above. The resulting  $J = 0.159(14)$  eV is to be compared with the  $2 \times 1 \times 1$  result of 0.16(3) eV. From this, we conclude that the finite size error must be within 0.03 eV, which is the statistical accuracy of the  $2 \times 1 \times 1$  calculations of Fig. 1 (c).

We would also like to give a brief comment here on the computational costs involved. The  $J$  values for  $2 \text{ eV} < U < 7 \text{ eV}$  in Fig. 3 (c) cost  $\sim 100\text{--}130\text{K}$  cpu hours each (error bar  $\sim 0.045$  eV). Calculating  $J$  for the  $2 \times 2 \times 1$  supercell took 1.8M cpu hours. We note that such costs are not insignificant, but are affordable on modern supercomputers such as Titan at ORNL.

In conclusion, we have presented a theoretical determination of the value of the spin superexchange constant in a transition metal oxide with the FP-DMC method. Our results for the 1D antiferromagnetic cuprate Ca<sub>2</sub>CuO<sub>3</sub> are in excellent agreement with experiment. Moreover, this is a purely *ab initio* approach, where the fixed phase error is controlled via the variational principle, with no empirical adjustable parameters. In this sense, FP-DMC

is superior to DFT where in order to improve the description of exchange and correlations one often resorts to LDA+U or hybrid functionals and chooses the “best” functional empirically. The success of FP-DMC in the present case implies that this method is capable of accurately describing the complicated spin superexchange processes between the correlated Cu 3*d* orbitals and oxygen 2*p* orbitals, involving on-site Coulomb correlations and *p*–*d* orbital hybridization. We hope that our present successful application of FP-DMC will stimulate future studies of magnetic and other properties of strongly correlated transition metal oxides with this highly competitive *ab initio* method.

Note: At the time of submitting this manuscript, we learned of similar DMC calculations, performed independently, published on [arXiv.org](https://arxiv.org) [33].

The authors would like to thank L. Shulenburg for sharing expertise in pseudopotential construction and for providing access to pseudopotential datasets prior to publication. The work was supported by the Materials Sciences & Engineering Division of the Office of Basic Energy Sciences, U.S. Department of Energy. PRCK was supported by the Scientific User Facilities Division, Office of Basic Energy Sciences, U.S. Department of Energy. Computational time used resources of the Oak Ridge Leadership Computing Facility at the Oak Ridge National Laboratory, which is supported by the Office of Science of the U.S. Department of Energy under Contract No. DE-AC05-00OR22725.

## Appendix A: Pseudopotential tests

For oxygen and calcium we used the pseudopotentials (PPs) optimized by Shulenburg and Mattsson [17], who also demonstrated their good quality by performing numerous tests. Of a much greater concern in the present study was the proper performance of the Cu PP since the magnetic properties of  $\text{Ca}_2\text{CuO}_3$  are largely determined by the behavior of the Cu 3*d* electrons. Therefore, we subjected our candidate Cu PPs to a comprehensive selection process, as presented below. The candidate Cu PPs were generated using the Opium code [34]. Our final choice is the hard Ne-core Cu PP [Fig. 3 (a), (c)] that satisfies the most stringent accuracy criteria and thus ensures the validity of the bulk calculations.

### 1. Bulk DFT calculations and rejection of Ar-core Cu pseudopotentials

Using our hard Ne-core Cu PP, we are able to accurately reproduce with Quantum Espresso the LDA results of the all-electron (AE) code WIEN2k [35] for bulk  $\text{Ca}_2\text{CuO}_3$  in an antiferromagnetic (AFM) and a ferromagnetic (FM) states. Thus, in Fig. 2 the  $\text{Ca}_2\text{CuO}_3$  densities of states (DOS) obtained from PP and AE calculations are compared, for an AFM [Fig. 2 (a)] and an

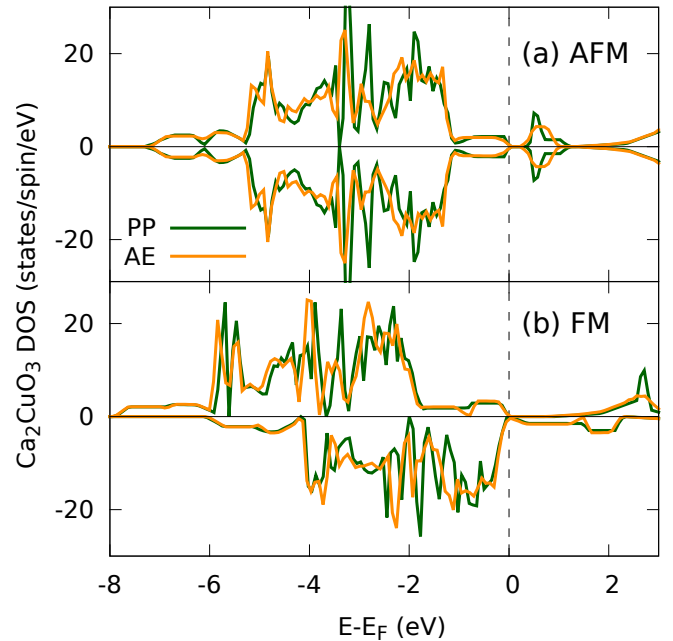


FIG. 2. The comparison of the  $\text{Ca}_2\text{CuO}_3$  densities of states (DOS) calculated using PP and AE codes: (a) antiferromagnetic and (b) ferromagnetic states. Energies are measured relative to the Fermi level  $E_F$ .

FM [Fig. 2 (b)] Cu spin configurations. For both configurations, the agreement with the AE code is very good. Interestingly, we were able to equally well reproduce the AE DOS when also using properly optimized Mg-core Cu PPs. This, however, did not hold for any of the Ar-core Cu PPs we tried: in this case, the bandwidth of the PP states as well as the conduction gap (AFM configuration) are systematically larger than in the AE calculations. This allowed us to discard Ar-core Cu PPs already at this stage of PP validation.

As for the spin superexchange coupling constant  $J$ , Quantum Espresso with the hard Ne-core Cu PP gives 0.64 eV in LDA, while WIEN2k gives 0.72 eV. In LDA+U, the WIEN2k  $J$  is rapidly decreasing as  $1/U$ . In PP DFT, we find only a weak dependence on  $U$ . This may be a peculiarity of the implementation of the LDA+U scheme within the plane-wave basis method of Quantum Espresso.

### 2. FP-DMC atom ionization energies and rejection of Mg-core Cu pseudopotentials

As we have pointed out, in DFT calculations for bulk  $\text{Ca}_2\text{CuO}_3$ , the Ne-core and the Mg-core Cu PPs appear to be equally good, provided proper optimization has been carried out. However, this does not necessarily mean that they will perform well in diffusion Monte Carlo calculations. In order to test the latter, we calculated the



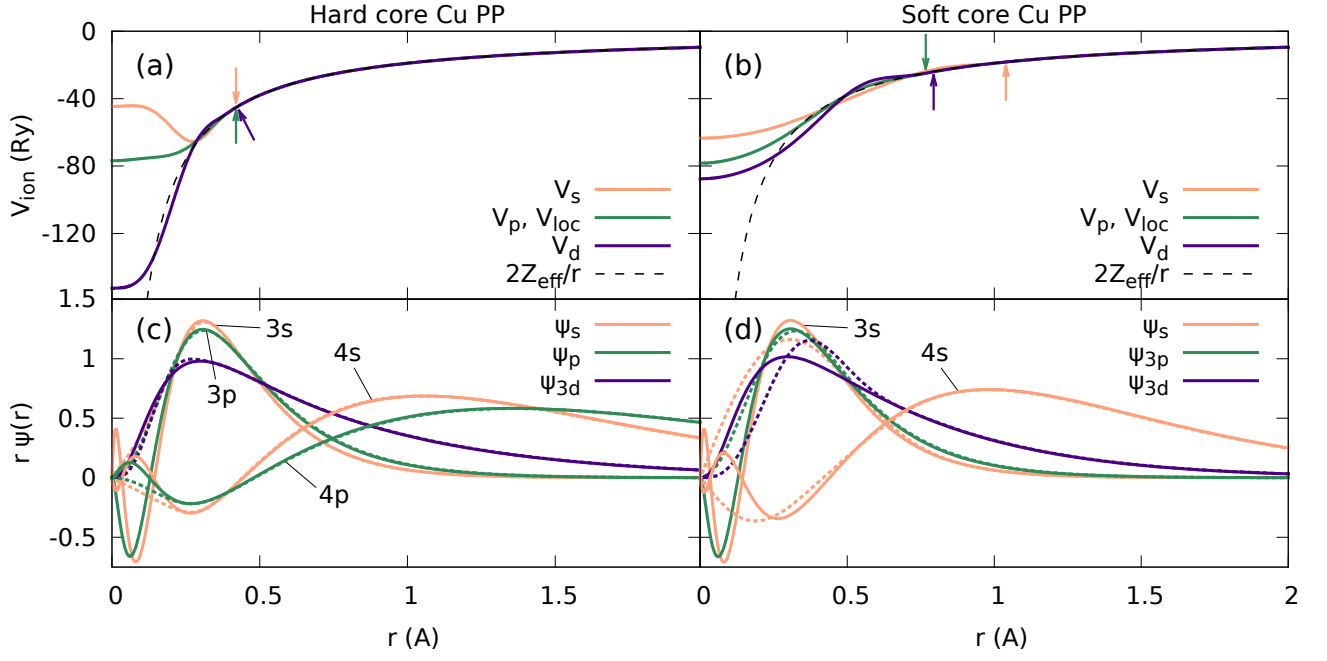


FIG. 3. (a) Hard and (b) soft Ne-core Cu pseudopotentials (PPs).  $V_{\text{loc}}$ ,  $V_s$ ,  $V_p$ , and  $V_d$  represent the local,  $s$ -,  $p$ -, and  $d$ -channels, respectively.  $2Z_{\text{eff}}/r$  represents the Coulomb potential due to the effective charge  $Z_{\text{eff}}$ . The arrowed lines of respective colors indicate cut-off radii for the three pseudopotential channels. (c), (d): The Cu atom eigenfunctions obtained in LDA with the hard (c) and soft (d) Ne-core Cu PPs. The solid (dashed) lines represent wave functions obtained from all-electron (PP) calculations.

Cu atom ionization energy with FP-DMC, using LDA for generating trial wave functions. The FP-DMC computational parameters are the following:  $3.125 \cdot 10^{-4} \text{ Ha}^{-1}$  for the imaginary time step and 4000 for the number of DMC walkers. With the hard Ne-core and with the Mg-core Cu PPs, we obtain, respectively, 7.724(37) eV and 8.302(36) eV for the Cu atom ionization energy. The former number is in a much better agreement with the experimental result of 7.72638(1) eV. One of the reasons of the poor performance of the Mg-core PP in this test, is that the 3s orbital, which is treated as core here, has a significant overlap in space with the 3p orbital, treated as valence [see Fig. 3 (c)]. This causes less trouble in DFT which is formulated in terms of Kohn-Sham orbitals so that such a division based on orbital character is natural. DMC, on the other hand, operates with a full many-electron wave function where a removal of the 3s electrons negatively affects the representation of the motion of the nearby 3p electrons. This issue has also been discussed in the context of GW [36, 37].

We would like to point out that using a Mg-core Cu PP instead of a Ne-core one in bulk  $\text{Ca}_2\text{CuO}_3$  FP-DMC calculations could provide a speedup of more than 30%, owing to the fact that the deeply lying 3s electrons are a significant source of the energy variance.

### 3. Equation of state of CuO dimer and hard vs. soft Ne-core Cu pseudopotentials

Although the hard Ne-core PP has been proven to be of a good quality for both DFT and DMC, it has a disadvantage in terms of computational load and memory demands as it requires a minimum of 500 Ry energy cut-off for the Quantum Espresso plane-wave basis. This results from the quite small cut-off radii of the  $s$ -,  $p$ -, and  $d$ -channels, as shown in Fig. 3 (a). In view of this, we constructed and tested an alternative Ne-core Cu PP with a soft core and low energy cut-off requirements of less than 200 Ry [Fig. 3 (b)]. It demonstrated excellent characteristics in DFT tests but, unfortunately, gives worse results in DMC than the hard-core Cu PP. In particular, with the soft-core PP the equilibrium interatomic separation distance in a CuO molecule is overestimated by more than 3% in FP-DMC [holds for LDA, LDA+U ( $U=3.5, 6$  eV), and B3LYP wave functions], whereas with the hard-core PP it is overestimated by only 0.6% (Fig. 4). Also the Cu atom ionization energy is slightly underestimated: 7.548(42) eV. Thus all calculations in DMC reported in the paper were obtained with the hard Ne-core pseudopotential. The surprising sensitivities to pseudopotential formulation that we find even for small core pseudopotentials indicates that careful testing is essential and results from large core pseudopotentials must be treated with caution.

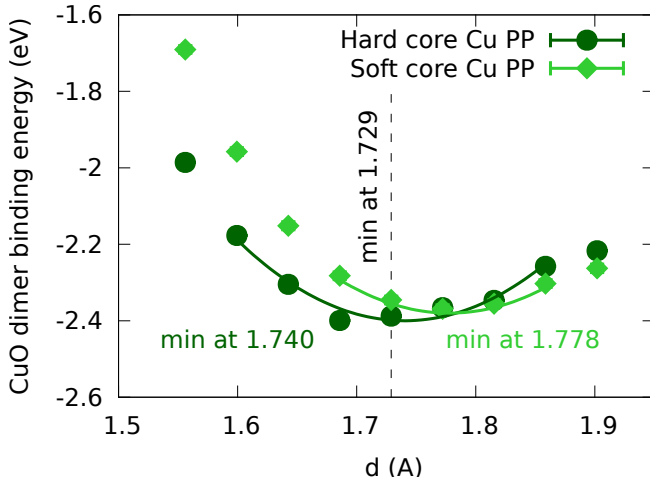


FIG. 4. Binding energy as a function of the interatomic separation  $d$  in a CuO dimer molecule. The vertical dashed line indicates the experimental equilibrium separation. The solid lines are a quadratic fit to the data.

- 
- [1] P. W. Anderson, *The Resonating Valence Bond State in  $\text{La}_2\text{CuO}_4$  and Superconductivity*, *Science* **235**, 1196 (1987).
- [2] D. Scalapino, *The case for  $d_{x^2-y^2}$  pairing in the cuprate superconductors*, *Phys. Rep.* **250**, 329 (1995).
- [3] E. Dagotto, *Correlated electrons in high-temperature superconductors*, *Rev. Mod. Phys.* **66**, 763 (1994).
- [4] O. Janson, *D cuprate microscopic magnetic modeling for low-dimensional spin systems*, Ph.D. thesis, Technische Universität Dresden, (2012).
- [5] A. C. Walters, T. G. Perring, J. Caux, A. T. Savici, G. D. Gu, C. Lee, W. Ku, and I. A. Zaliznyak, *Effect of covalent bonding on magnetism and the missing neutron intensity in copper oxide compounds*, *Nat. Phys.* **5**, 867 (2009).
- [6] T. Ami, M. K. Crawford, R. L. Harlow, Z. R. Wang, D. C. Johnston, Q. Huang, and R. W. Erwin, *Magnetic susceptibility and low-temperature structure of the linear chain cuprate  $\text{Sr}_2\text{CuO}_3$* , *Phys. Rev. B* **51**, 5994 (1995).
- [7] S. Eggert, *Accurate determination of the exchange constant in  $\text{Sr}_2\text{CuO}_3$  from recent theoretical results*, *Phys. Rev. B* **53**, 5116 (1996).
- [8] N. Motoyama, H. Eisaki, and S. Uchida, *Magnetic Susceptibility of Ideal Spin 1/2 Heisenberg Antiferromagnetic Chain Systems,  $\text{Sr}_2\text{CuO}_3$  and  $\text{SrCuO}_2$* , *Phys. Rev. Lett.* **76**, 3212 (1996).
- [9] Associating the QMC AFM state with the Bethe ansatz ground-state of the 1D Heisenberg model (instead of the N'eel/Ising state as is usually done [24–29]) gives a different representation of  $J$ :  $J \approx 0.72J^{\text{N'eel}} = 0.115(10)$  eV.
- [10] C. de Graaf and F. Illas, *Electronic structure and magnetic interactions of the spin-chain compounds  $\text{Ca}_2\text{CuO}_3$  and  $\text{Sr}_2\text{CuO}_3$* , *Phys. Rev. B* **63**, 014404 (2000).
- [11] J. Schlappa, K. Wohlfeld, K. J. Zhou, M. Mourigal, M. W. Haverkort, V. N. Strocov, L. Hozoi, C. Monney, S. Nishimoto, S. Singh, A. Revcolevschi, J. Caux, L. Patthey, H. M. Rønnow, J. van den Brink, and T. Schmitt, *Spinorbital separation in the quasi-one-dimensional Mott insulator  $\text{Sr}_2\text{CuO}_3$* , *Nature* **485**, 82 (2012).
- [12] From the fit to the temperature dependence of magnetic susceptibility, the superexchange constant  $J$  between the nearest-neighbor Cu spins in  $\text{Sr}_2\text{CuO}_3$  was estimated as 0.146(13) [7] and 0.189(17) [8] eV. For the same compound, analysis of the angle-resolved photoemission spectroscopy data leads to a  $J$  value between 0.13 and 0.16 eV [38] while the midinfrared spectrum interpretation in terms of phonon-assisted magnetic excitations to a value between 0.246 and 0.26 eV [39, 40]. Resonant inelastic x-ray scattering [11] and inelastic neutron scattering [5] data point to 0.249 and 0.241(11) eV, respectively. Finally, from the  $^{63}\text{Cu}$  neutron magnetic resonance data one infers the  $J$  value of 0.24 eV [41, 42].
- [13] S. Eggert, I. Affleck, and M. Takahashi, *Susceptibility of the spin 1/2 Heisenberg antiferromagnetic chain*, *Phys. Rev. Lett.* **73**, 332 (1994).
- [14] W. M. C. Foulkes, L. Mitás, R. J. Needs, and G. Rajagopal, *Quantum Monte Carlo simulations of solids*, *Rev. of Mod. Phys.* **73**, 33 (2001).
- [15] C. L. Teske and H. Müller-Buschbaum, *Über Erdalkalimetall-Oxocuprate. IV. Zur Kenntnis von  $\text{SrCu}_2\text{O}_2$* , *Z. Anorg. Allg. Chem.* **379**, 113 (1970).
- [16] D. M. Ceperley and B. J. Alder, *Ground State of the Electron Gas by a Stochastic Method*, *Phys. Rev. Lett.* **45**, 566 (1980).

- [17] L. Shulenburger and T. R. Mattsson, *Quantum Monte Carlo applied to solids*, *Phys. Rev. B* **88**, 245117 (2013).
- [18] G. H. Booth, A. Grüneis, G. Kresse, and A. Alavi, *Towards an exact description of electronic wavefunctions in real solids*, *Nature* **493**, 365 (2013).
- [19] R. Q. Hood, P. R. C. Kent, and F. A. Reboredo, *Diffusion quantum Monte Carlo study of the equation of state and point defects in aluminum*, *Phys. Rev. B* **85**, 134109 (2012).
- [20] K. P. Esler, R. E. Cohen, B. Militzer, J. Kim, R. J. Needs, and M. D. Towler, *Fundamental High-Pressure Calibration from All-Electron Quantum Monte Carlo Calculations*, *Phys. Rev. Lett.* **104**, 185702 (2010).
- [21] L. Spanu, S. Sorella, and G. Galli, *Nature and Strength of Interlayer Binding in Graphite*, *Phys. Rev. Lett.* **103**, 196401 (2009).
- [22] J. Kolorenč and L. Mitas, *Quantum Monte Carlo Calculations of Structural Properties of FeO Under Pressure*, *Phys. Rev. Lett.* **101**, 185502 (2008).
- [23] P. Giannozzi, S. Baroni, N. Bonini, M. Calandra, R. Car, C. Cavazzoni, D. Ceresoli, G. L. Chiarotti, M. Cococcioni, I. Dabo, A. Dal Corso, S. de Gironcoli, S. Fabris, G. Fratesi, R. Gebauer, U. Gerstmann, C. Gougousis, A. Kokalj, M. Lazzeri, L. Martin-Samos, N. Marzari, F. Mauri, R. Mazzarello, S. Paolini, A. Pasquarello, L. Paulatto, C. Sbraccia, S. Scandolo, G. Sclauzero, A. P. Seitsonen, A. Smogunov, P. Umari, and R. M. Wentzcovitch, *QUANTUM ESPRESSO: a modular and open-source software project for quantum simulations of materials*, *J. Phys.: Condens. Matter* **21**, 395502 (2009).
- [24] I. I. Mazin, M. D. Johannes, L. Boeri, K. Koepernik, and D. J. Singh, *Problems with reconciling density functional theory calculations with experiment in ferropernictides*, *Phys. Rev. B* **78**, 085104 (2008).
- [25] F. Ma, Z. Lu, and T. Xiang, *Arsenic-bridged antiferromagnetic superexchange interactions in LaFeAsO*, *Phys. Rev. B* **78**, 224517 (2008).
- [26] H. Akamatsu, Y. Kumagai, F. Oba, K. Fujita, H. Murakami, K. Tanaka, and I. Tanaka, *Antiferromagnetic superexchange via 3d states of titanium in EuTiO<sub>3</sub> as seen from hybrid Hartree-Fock density functional calculations*, *Phys. Rev. B* **83**, 214421 (2011).
- [27] H. Seo, A. Posadas, and A. A. Demkov, *Strain-driven spin-state transition and superexchange interaction in LaCoO<sub>3</sub>: Ab initio study*, *Phys. Rev. B* **86**, 014430 (2012).
- [28] C. Duan, R. F. Sabiryanov, W. N. Mei, P. A. Dowben, S. S. Jaswal, and E. Y. Tsymbal, *Magnetic ordering in Gd monopnictides: Indirect exchange versus superexchange interaction*, *Appl. Phys. Lett.* **88**, (2006).
- [29] P. Reinhardt, M. P. Habas, R. Dovesi, I. de P. R. Moreira, and F. Illas, *Magnetic coupling in the weak ferromagnet CuF<sub>2</sub>*, *Phys. Rev. B* **59**, 1016 (1999).
- [30] D. Ceperley, *Fermion nodes*, *J. Stat. Phys.* **63**, 1237 (1991).
- [31] J. Kim, K. P. Esler, J. McMinis, M. A. Morales, B. K. Clark, L. Shulenburger, and D. M. Ceperley, *Hybrid algorithms in quantum Monte Carlo*, *J. Phys. Conf. Ser.* **402**, 012008 (2012).
- [32] H. Rosner, *Electronic structure and exchange integrals of low-dimensional cuprates*, Ph.D. thesis, Technische Universität Dresden, (1999).
- [33] L. K. Wagner and P. Abbamonte, *The effect of electron correlation on the electronic structure and spin-lattice coupling of the high-T<sub>c</sub> cuprates: quantum Monte Carlo calculations*, *arXiv:1402.4680* (2014).
- [34] E. Walter, *OPIUM*, <http://opium.sourceforge.net>
- [35] P. Blaha, K. Schwarz, G. K. H. Madsen, D. Kvasnicka, and J. Luitz, *WIEN2K, An Augmented Plane Wave + Local Orbitals Program for Calculating Crystal Properties*, Karlheinz Schwarz, Techn. Universität Wien, Austria, (2001).
- [36] H. Dixit, R. Saniz, D. Lamoen, and B. Partoens, *The quasiparticle band structure of zincblende and rocksalt ZnO*, *J. Phys.: Condens. Matter* **22**, 125505 (2010).
- [37] H. Dixit, R. Saniz, D. Lamoen, and B. Partoens, *Accurate pseudopotential description of the GW bandstructure of ZnO*, *Comput. Phys. Commun.* **182**, 2029 (2011).
- [38] H. Fujisawa, T. Yokoya, T. Takahashi, S. Miyasaka, M. Kibune, and H. Takagi, *Spin-charge separation in single-chain compound Sr<sub>2</sub>CuO<sub>3</sub> studied by angle-resolved photoemission*, *Solid State Commun.* **106**, 543 (1998).
- [39] J. Lorenzana and R. Eder, *Dynamics of the one-dimensional Heisenberg model and optical absorption of spinons in cuprate antiferromagnetic chains*, *Phys. Rev. B* **55**, R3358 (1997).
- [40] H. Suzuura, H. Yasuhara, A. Furusaki, N. Nagaosa, and Y. Tokura, *Singularities in Optical Spectra of Quantum Spin Chains*, *Phys. Rev. Lett.* **76**, 2579 (1996).
- [41] M. Takigawa, O. A. Starykh, A. W. Sandvik, and R. R. P. Singh, *Nuclear relaxation in the spin-1/2 antiferromagnetic chain compound Sr<sub>2</sub>CuO<sub>3</sub>: Comparison between theories and experiments*, *Phys. Rev. B* **56**, 13681 (1997).
- [42] M. Takigawa, N. Motoyama, H. Eisaki, and S. Uchida, *Dynamics in the S = 1/2 One-Dimensional Antiferromagnet Sr<sub>2</sub>CuO<sub>3</sub> via <sup>63</sup>Cu NMR*, *Phys. Rev. Lett.* **76**, 4612 (1996).